

# Emissivity measurement under vacuum in the wavelength range from 4 $\mu\text{m}$ to 100 $\mu\text{m}$ and temperature range from -40 $^{\circ}\text{C}$ to 500 $^{\circ}\text{C}$ at PTB

*A. Adibekyan<sup>1</sup>, C. Monte<sup>1</sup>, M. Kehrt<sup>1</sup>, B. Gutschwager<sup>1</sup>, J. Hollandt<sup>1</sup>*

<sup>1</sup> *Physikalisch-Technische Bundesanstalt (PTB), Abbestr. 2-12, D-10587 Berlin, Germany, albert.adibekyan@ptb.de*

## Abstract

A new facility of the Physikalisch-Technische Bundesanstalt (PTB) for emissivity measurement under vacuum was brought into operation capable to measure directional spectral emissivity in the wavelength range from 4  $\mu\text{m}$  to 100  $\mu\text{m}$  and temperature range from -40  $^{\circ}\text{C}$  to 500  $^{\circ}\text{C}$ . Here we present the measurement scheme with respect to the spectral radiance of two blackbodies at different temperatures and discuss the evaluation of the emissivity results.

We present first results of emissivity measurements under vacuum in the wavelength range from 4  $\mu\text{m}$  to 100  $\mu\text{m}$  and temperature range from -20  $^{\circ}\text{C}$  to 200  $^{\circ}\text{C}$ , compare them with results obtained in air and show that samples with very low emissivity can be measured with sufficiently low uncertainty.

**Key words:** emissivity, vacuum, blackbody, spectral radiance, uncertainty.

## Introduction

The accurate knowledge of the emissivity of a material is of large interest for different technological applications. Examples of vacuum applications which require very low uncertainties of emissivity are absorbers for solar thermal electricity generation [1] and coatings of onboard reference blackbodies for benchmark missions in space [2].

With the new PTB facility the emissivity of samples can be measured under vacuum conditions in the wavelength range from 4  $\mu\text{m}$  to 100  $\mu\text{m}$  and temperature range from -40  $^{\circ}\text{C}$  to 500  $^{\circ}\text{C}$ . In the Reduced Background Calibration Facility (RBCF) [3] at PTB all critical components of the optical path are cooled with liquid nitrogen (see Fig. 1). Hereby the background radiation is largely reduced and consequently the uncertainty of emissivity measurements is reduced too.

## Calculation of emissivity

The measurement scheme is based on a comparison of the spectral radiance of a sample inside of a temperature stabilized spherical enclosure with the spectral radiances of two reference blackbodies at different temperatures. The emissivity can be obtained from the ratio:

$$Q = \frac{\tilde{L}_{\text{Sample}}(T_{\text{Sample}}) - \tilde{L}_{\text{BB-LN}_2}(T_{\text{BB-LN}_2})}{\tilde{L}_{\text{BB1}}(T_{\text{BB1}}) - \tilde{L}_{\text{BB-LN}_2}(T_{\text{BB-LN}_2})} \quad (1)$$

Where  $\tilde{L}_{\text{Sample}}(T_{\text{Sample}})$  denotes the signal measured from the sample,  $\tilde{L}_{\text{BB1}}(T_{\text{BB1}})$  the signal from the first ("main") blackbody and  $\tilde{L}_{\text{BB-LN}_2}(T_{\text{BB-LN}_2})$  the signal from the second blackbody, respectively. As the "main" blackbody we use either the vacuum low-temperature blackbody (VLTBB) [4] or the vacuum medium-temperature blackbody (VMTBB) [5] depending on the temperature range. The "main" blackbody is usually operated at the temperature of the sample or close to it. The measured signal  $\tilde{L}_{\text{BB1}}(T_{\text{BB1}})$  of this blackbody is given by:

$$\tilde{L}_{\text{BB1}}(T_{\text{BB1}}) = s(L_{\text{BB1}}(T_{\text{BB1}}) + L_{\text{Background}} - L_{\text{Detector}}) \quad (2)$$

The spectral radiance of the blackbody is given by  $L_{\text{BB1}}(T_{\text{BB1}}) = \varepsilon_{\text{BB1}} L_{\text{Planck}}(T_{\text{BB1}})$ , where  $L_{\text{Planck}}(T_{\text{BB1}})$  is the spectral blackbody radiance at the respective temperature given by Planck's law and  $\varepsilon_{\text{BB1}}$  is the directional spectral effective emissivity of the blackbody.

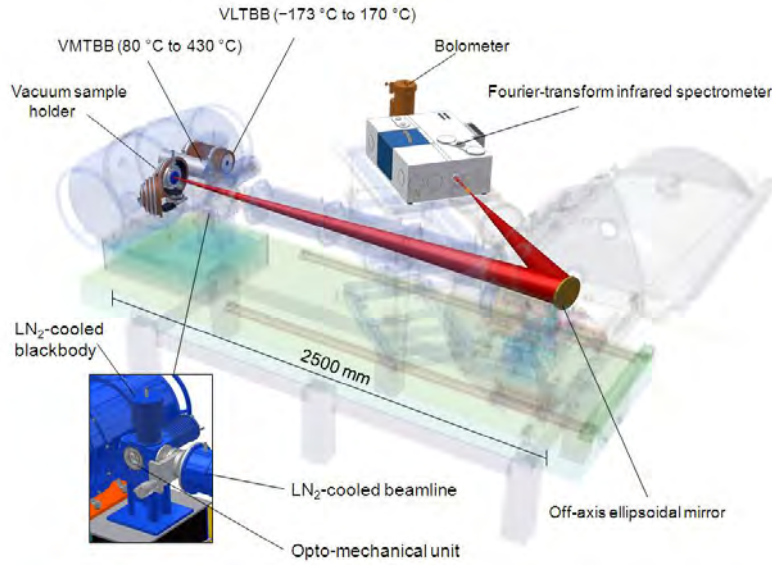


Fig. 1. Transparent view of the Reduced Background Calibration Facility (RBCF) shows the two vacuum blackbodies VLTBB and VMTBB, the sample holder for emissivity measurements, the LN<sub>2</sub>-cooled reference blackbody, the Fourier-transform spectrometer and the optical path of the radiation in the LN<sub>2</sub>-cooled beamline.

$L_{\text{Background}}$  denotes the spectral radiance of the thermal background of the RBCF and  $L_{\text{Detector}}$  the spectral radiance of the detector. The value  $s$  is the spectral responsivity of the spectrometer.

The second reference source in our experiment, the LN<sub>2</sub>-cooled blackbody, is mounted on top of the opto-mechanical unit (see Fig. 1) and is used for the elimination of the background radiation. Its measured signal is given by:

$$\tilde{L}_{\text{BB-LN}_2}(T_{\text{BB-LN}_2}) = s(\rho_{\text{Chopper}} L_{\text{BB-LN}_2}(T_{\text{BB-LN}_2}) + L_{\text{Chopper}}(T_{\text{Chopper}}) + L_{\text{Background}} - L_{\text{Detector}}) \quad (3)$$

The changes with respect to eq. (2) are the additional radiance of the highly reflective chopper  $L_{\text{Chopper}}(T_{\text{Chopper}}) = \varepsilon_{\text{Chopper}} L_{\text{Planck}}(T_{\text{Chopper}})$

and its directional spectral reflectance  $\rho_{\text{Chopper}}$  which is due to the design of the RBCF, where the chopper is used to image the radiance of the cold-reference blackbody onto the optical axis.

By forming the difference of equations (2) and (3) the terms of the background radiance  $L_{\text{Background}}$  and the detector radiance  $L_{\text{Detector}}$  can be eliminated:

$$\tilde{L}_{\text{BB1}}(T_{\text{BB1}}) - \tilde{L}_{\text{BB-LN}_2}(T_{\text{BB-LN}_2}) = s(L_{\text{BB1}}(T_{\text{BB1}}) - \rho_{\text{Chopper}} L_{\text{BB-LN}_2}(T_{\text{BB-LN}_2}) - L_{\text{Chopper}}(T_{\text{Chopper}})) \quad (4)$$

The recorded signal of the sample  $\tilde{L}_{\text{Sample}}(T_{\text{Sample}})$  results not only from the radiation

emitted directly by the sample, the background radiance and the detector radiance as it is the case when observing the two blackbodies. Additionally, the radiation emitted by the enclosure of the sample  $\varepsilon_{\text{Encl.}} L_{\text{Planck}}(T_{\text{Encl.}})$ , which is reflected towards the detector by the directional-hemispherical reflectance of the sample  $\rho_{\text{Sample}} = 1 - \varepsilon_{\text{Sample}}$  has to be considered.

$$\begin{aligned} \tilde{L}_{\text{Sample}}(T_{\text{Sample}}) - \tilde{L}_{\text{BB-LN}_2}(T_{\text{BB-LN}_2}) &= \\ &= s(\varepsilon_{\text{Sample}} L_{\text{Planck}}(T_{\text{Sample}}) + (1 - \varepsilon_{\text{Sample}}) \varepsilon_{\text{Encl.}} L_{\text{Planck}}(T_{\text{Encl.}}) - \\ &\quad - \rho_{\text{Chopper}} \varepsilon_{\text{BB-LN}_2} L_{\text{Planck}}(T_{\text{BB-LN}_2}) - \varepsilon_{\text{Chopper}} L_{\text{Planck}}(T_{\text{Chopper}})) \end{aligned} \quad (5)$$

Furthermore, for highly reflecting and hence low emitting samples the radiation emitted by the sample into the spherical enclosure which is then partly reflected back by the enclosure and via the directional-hemispherical reflectance of the sample partly reflected towards the detector has to be considered as well. For the latter case and for the radiation originating from the sphere multiple reflections can occur [6]. Depending on the sample properties their magnitude can be significant and then has to be considered. However, this leads to a complicate expression with multiple sums which is omitted here for clarity.

Finally the background corrected signals from the blackbody (eq. 4) and the sample (eq. 5) (or the here not explicitly given expression considering multiple reflections) are substituted into the ratio (1) which is then solved for the emissivity of the sample. Since all temperatures and all other relevant quantities in the derived

expression are recorded or known [7] during the experiment the emissivity can be calculated.

### Experimental results

As an example in Figure 2 measurements under vacuum of the spectral directional emissivity of silicon carbide at different temperatures are compared. Both measurements were recorded with a room temperature detector. The measurement

at  $-20\text{ }^{\circ}\text{C}$  exhibits a higher noise level but shows no systematic deviations to the measurement at  $200\text{ }^{\circ}\text{C}$  within the range of the expanded measurement uncertainty. The temperature variation of the emissivity of SiC is negligible within the uncertainty in this temperature range. So the result illustrates the ability to determine emissivities below  $0\text{ }^{\circ}\text{C}$  correctly.

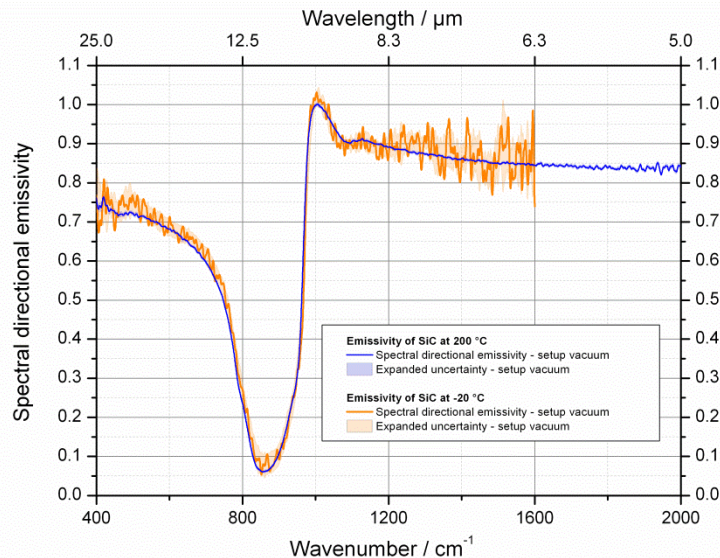


Fig. 2. The spectral directional emissivity of a SiC sample measured under vacuum at temperatures of  $-20\text{ }^{\circ}\text{C}$  and  $200\text{ }^{\circ}\text{C}$ .

Further examples are given in Figures 3 and 4, where we show the emissivity of a gold mirror within the range of the expanded uncertainty of this measurement. A gold mirror is an excellent example of a material with very low emissivity and hence a critical assessment of the capabilities of the RBCF and a test for the suggested method of calculation to determine the emissivity. The directional spectral emissivity of the gold mirror was measured under vacuum at a polar angle of  $15^{\circ}$  and a temperature of  $200\text{ }^{\circ}\text{C}$ . In Figure 3 the emissivity measurement under vacuum is compared with a measurement of the same sample at the same temperature performed at the setup under air at PTB [8, 9]. Both measurements are compared to an emissivity determined indirectly from a specular reflectivity measurement of the same sample. All three results agree well within their range of

uncertainty. The measurement under air shows artefacts around  $1600\text{ cm}^{-1}$  caused by residual water absorption. These artefacts are absent under vacuum, hence the emissivity measurements are undisturbed in this range and the systematic uncertainty is reduced.

Furthermore, the hemispherical total emissivity of a sample can be determined at the RBCF from a sequence of measurements at different polar angles of the sample. As an example the spectral directional emissivity of the gold mirror is shown at angles from  $15^{\circ}$  to  $70^{\circ}$  in Figure 4. The resulting integrated quantities, the total directional emissivities and the total hemispherical emissivity, which were calculated from the spectral quantities are shown in the inset.



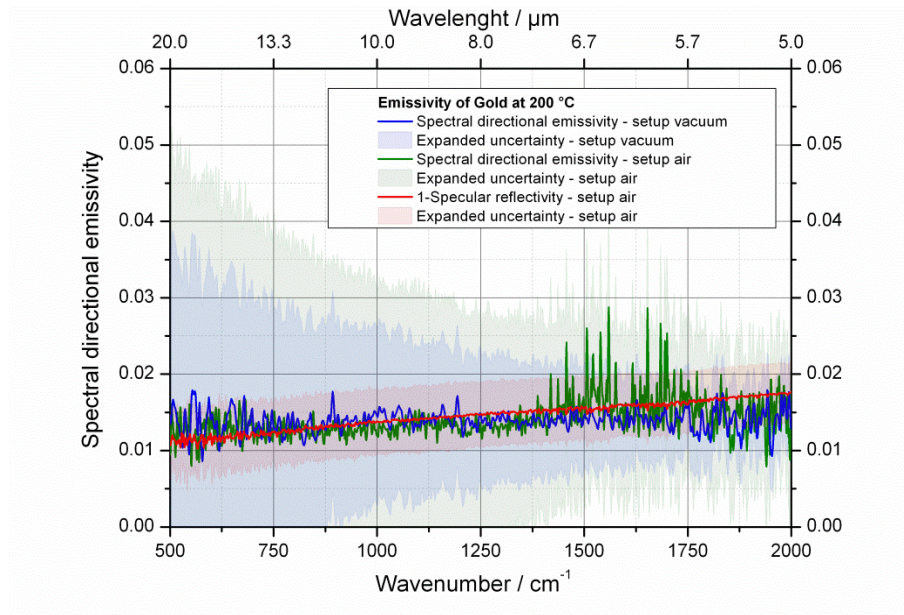


Fig. 3. The spectral directional emissivity of a low-emitting gold sample measured at the setup under vacuum and at the setup under air at a temperature of 200 °C compared with the indirectly determined emissivity from a specular reflectance measurement.

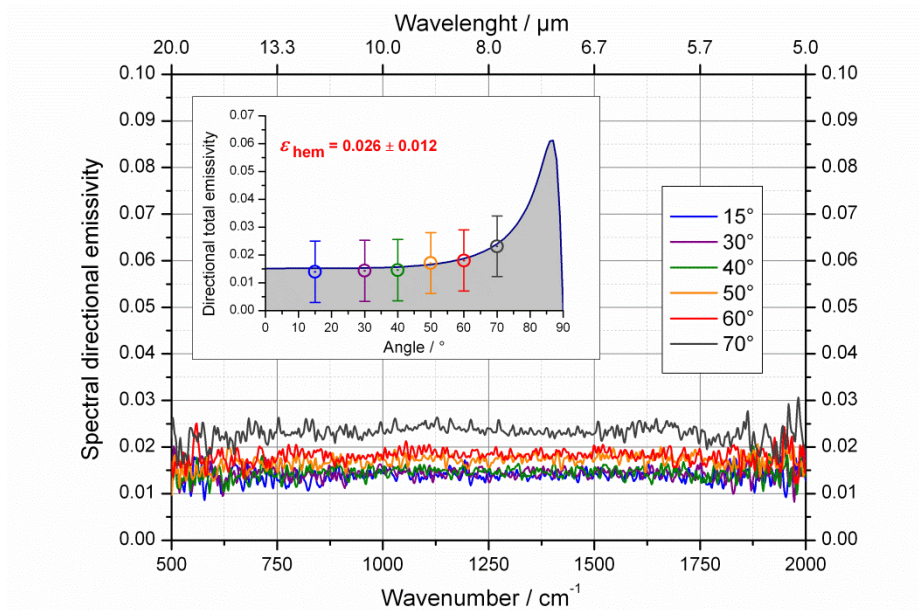


Fig. 4. The spectral directional emissivity of a gold mirror measured at different polar angles. The resulting values for the total directional emissivities and the total hemispherical emissivity  $\epsilon_{\text{hem}}$  are shown in the inset.

In Figure 5 we present our first results of emissivity measurements under vacuum in the wavelength range up to 100  $\mu\text{m}$ . The spectral directional emissivity of the black paint Aeroglaze Z306 was measured under vacuum at a temperature of 150 °C and compared in the overlapping wavelength range from 16.7  $\mu\text{m}$  to 25  $\mu\text{m}$  with a measurement performed at the emissivity setup in air at PTB. At the setup in air the spectrometer was equipped with a pyroelectric DLaTGS detector and a KBr broadband beamsplitter. At the setup under

vacuum a pyroelectric FDTGS detector and a Multilayer beamsplitter were used. The results show a good agreement within the range of uncertainty. Additionally the specular reflectivity (geometry 12°/12°) of this sample has been determined and is plotted in the form of “1-specular reflectivity”. The difference between the two curves corresponds to the diffusive term of the directional hemispherical reflectivity which becomes smaller towards longer wavelength.

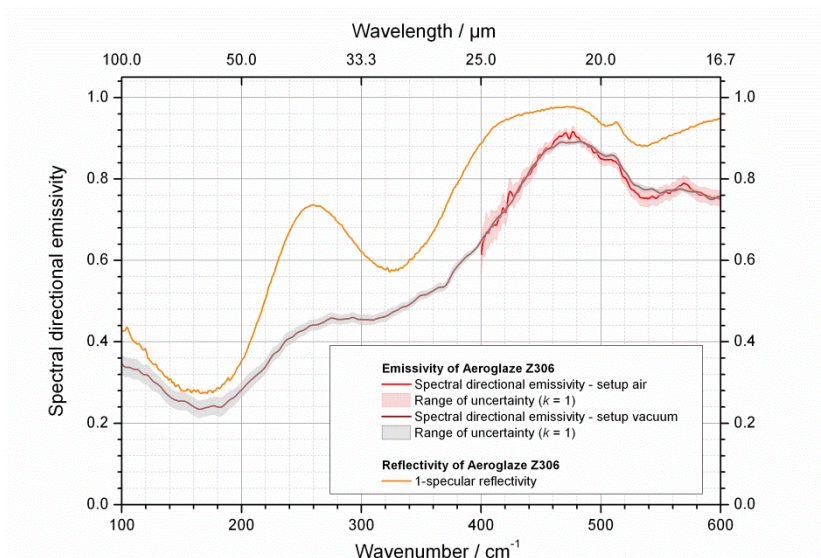


Fig. 5. The spectral directional emissivity of the black paint Aeroglaze Z306 measured at the setup under vacuum up to 100  $\mu\text{m}$  and compared with a measurement performed at the setup in air in the overlapping wavelength range from 16.7  $\mu\text{m}$  to 25  $\mu\text{m}$ . Additionally the spectral directional reflectivity of the same sample is shown in the form of “1-specular reflectivity”.

## Conclusion

The PTB has started to perform highly accurate directional spectral emissivity measurement under vacuum in the wavelength range from 4  $\mu\text{m}$  to 100  $\mu\text{m}$  and temperature range from  $-40\text{ }^{\circ}\text{C}$  to  $500\text{ }^{\circ}\text{C}$  at the Reduced-Background Calibration Facility (RBCF). The scheme for direct emissivity measurements under vacuum is based on the measurement of the spectral radiance of a sample inside of a temperature stabilized spherical enclosure with respect to the spectral radiance of two reference blackbodies at different temperatures. The evaluation procedure for low emitting samples has to take into account multiple reflections between the hemispherical enclosure and the sample.

The measurements under vacuum show a good agreement with the measurements performed at the setup in air. They exhibit smaller systematic uncertainties resulting from the operation under vacuum conditions, and the cooling of all critical parts with liquid nitrogen. Due to the use of the enhanced evaluation scheme samples with very low emissivities can be measured with sufficient accuracy.

## References

- [1] C. E. Kennedy, Review of Mid- to High-Temperature Solar Selective Absorber Materials, National Renewable Energy Lab., Golden, CO. (US), Technical report (2002), doi: 10.2172/15000706
- [2] H. Latvakoski, M. Watson, S. Topham, D. Scott, M. Wojcik, G. Bingham, A high-accuracy

blackbody for CLARREO, Proc. of SPIE, 7808, Infrared Remote Sensing and Instrumentation XVIII, 2010, 78080X-78080X-12; doi: 10.1117/12.859477

- [3] C. Monte, B. Gutschwager, S. Morozova, and J. Hollandt, International Journal of Thermophysics Vol. 30, 203-219 (2009); doi: 10.1007/s10765-008-0442-9
- [4] S.P. Morozova et al., International Journal of Thermophysics Vol. 29, 341-351 (2008); doi: 10.1007/s10765-007-0355-z
- [5] S.P. Morozova et al., International Journal of Thermophysics Vol. 31, 1809-1820, (2010); doi: 10.1007/s10765-010-0843-4
- [6] Raúl B. Pérez-Sáez, Leire del Campo, Manuel J. Tello, Int J Thermophys (2008) 29, 1141–1155; doi: 10.1007/s10765-008-0402-4
- [7] A. Adibekyan et al. Measurement Techniques, Vol. 55, 1163-1171, (2013) doi:10.1007/s11018-012-0103-z
- [8] C. Monte, and J. Hollandt, High Temperatures - High Pressures Vol. 39, 151-164, (2010).
- [9] C. Monte, and J. Hollandt, Metrologia Vol. 47, S172-S181, (2010); doi: 10.1088/0026-1394/47/2/S14